

Phase diagram of H₂ adsorbed on graphene

M.C. Gordillo¹ and J. Boronat²

¹*Departamento de Sistemas Físicos, Químicos y Naturales,
Facultad de Ciencias Experimentales, Universidad Pablo de Olavide,
Carretera de Utrera, km 1. 41013 Sevilla, Spain*

²*Departament de Física i Enginyeria Nuclear, Universitat Politècnica
de Catalunya, Campus Nord B4-B5, 08034 Barcelona, Spain*

(Dated: October 29, 2018)

The phase diagram of the first layer of H₂ adsorbed on top of a single graphene sheet has been calculated by means of a series of diffusion Monte Carlo (DMC) simulations. We have found that, as in the case of ⁴He, the ground state of molecular hydrogen is a $\sqrt{3} \times \sqrt{3}$ commensurate structure, followed, upon a pressure increase, by an incommensurate triangular solid. A striped phase of intermediate density was also considered, and found lying on top of the equilibrium curve separating both commensurate and incommensurate solids.

I. INTRODUCTION

Graphene is a novel form of carbon, in which the atoms are located in the nodes of a honeycomb lattice that extends periodically in two dimensions forming a single layer.^{1,2} In this respect, graphene is different from graphite, a substrate formed by the superposition of these layers to build a complete three dimensional structure. Graphene can be obtained as a free standing structure,² or as a single adsorbed layer on top of another substrate.³ One of the main interests of the scientific community on graphene is related to its unusual electron transport properties that are determined by the Dirac equation,⁴⁻⁷ but other characteristics of this compound as for instance its behavior as adsorber are starting to be payed attention to. A recent diffusion Monte Carlo (DMC) calculation of ⁴He on graphene indicates that its behavior is quite similar to the one on graphite, the main difference being the binding energy, lower in the case of a single carbon sheet.⁸ It was also found⁸ that the ground state of helium on graphene is a $\sqrt{3} \times \sqrt{3}$ commensurate solid, in agreement with experimental data on graphite.^{9,10} The aim of the present work is to calculate the phase diagram of H₂ adsorbed on graphene at zero temperature using for the first time the DMC method. The comparison with the case of graphite will show us if there is any significant difference between them or graphene is simply a weaker binding version of the graphite phase diagram, as happens with ⁴He.

II. METHOD

Our study is based on the DMC method, basically because this technique allow us to obtain the correct ground state for a given system of bosons.¹¹ This is the case here, since we will consider only para-H₂, the ground state of the hydrogen molecule. An important ingredient of any DMC calculation is the trial wave function used for importance sampling. This function collects basic information about the system that is known *a priori*, and can

be considered a reasonable approximation (in the variational sense) to its ground state. In this work, we use as a initial trial wave function

$$\Phi(\mathbf{r}_1, \mathbf{r}_2, \dots, \mathbf{r}_N) = \prod_{i < j} \exp \left[-\frac{1}{2} \left(\frac{b_{\text{H}_2\text{-H}_2}}{r_{ij}} \right)^5 \right] \quad (1) \\ \times \prod_i \prod_J \exp \left[-\frac{1}{2} \left(\frac{b_{\text{C-H}_2}}{r_{iJ}} \right)^5 \right] \prod_i \exp(-a(z_i - z_0)^2),$$

that depends on the coordinates of the hydrogen molecules $\mathbf{r}_1, \mathbf{r}_2, \dots, \mathbf{r}_N$ and the position of the Carbon atoms \mathbf{r}_J of the substrate. The first term in Eq. (1) is a two-body Jastrow function depending on the H₂ intermolecular distances r_{ij} , with optimal parameter $b_{\text{H}_2\text{-H}_2} = 3.195 \text{ \AA}$. The second term is another Jastrow function that takes into account all the individual C-H₂ interactions, the optimal value of $b_{\text{C-H}_2}$ being 2.3 \AA . Finally, the third term is a product of one-body Gaussians that depend only on the z coordinate of each molecule and whose function is to localize the molecules near the z_0 value where the binding energy formed by the summing up of all the carbon-hydrogen interaction in the graphene-adsorbate system is larger. It depends on two parameters, whose optimal values are $a = 3.06 \text{ \AA}^{-2}$ and $z_0 = 2.9 \text{ \AA}$. All the parameters in the trial wave function (1) were variationally optimized for a liquid phase at density 0.0068 \AA^{-2} and their slight density dependence was neglected.

In the case of the different solid phases considered in this work, the trial function above (1) was multiplied by another set of Gaussians of the form

$$\prod_i \exp\{-c[(x_i - x_{\text{site}})^2 + (y_i - y_{\text{site}})^2]\} \quad (2)$$

i.e., each particle was limited to be in a region around its corresponding $x_{\text{site}}, y_{\text{site}}$ coordinates (Nosanow-Jastrow model). These coordinates corresponded to the crystallographic positions of the particular solid considered, and the parameter c was variationally optimized for each lattice type. For instance, for all the commensurate phases

TABLE I: Equilibrium density ρ_0 and energy per H_2 molecule at equilibrium e_0 for the liquid phase. Graphene (2D) and graphite (2D) indicate the results after the subtraction of their respective energies in the infinite dilution limit. 2D are DMC results for a strictly 2D H_2 system with the same intermolecular potential (Ref. 16). The spinodal densities ρ_s for the same systems are also shown.

	Graphene	Graphite	Graphene (2D)	Graphite (2D)	2D
e_0 (K)	-451.88 ± 0.03	-503.0 ± 0.1	-20.09 ± 0.07	-20.4 ± 0.1	-21.43 ± 0.02
ρ_0 (\AA^{-2})	0.05948 ± 0.00005	0.0593 ± 0.0004	0.05948 ± 0.00005	0.0593 ± 0.0004	0.0633 ± 0.0003
ρ_s (\AA^{-2})	0.0489 ± 0.0001	0.0486 ± 0.0001	0.0489 ± 0.0001	0.0486 ± 0.0001	-

considered in this work, $c = 0.61 \text{\AA}^{-2}$. For the incommensurate solid, a linear fit between the values obtained at densities 0.1 ($c = 1.38 \text{\AA}^{-2}$) and 0.08\AA^{-2} ($c = 0.61 \text{\AA}^{-2}$) was used. Below the latter density, c was kept fixed to 0.61\AA^{-2} . We used the Silvera and Goldman potential¹² for the H_2 - H_2 interaction, one of the standard potentials in Monte Carlo calculations of para- H_2 . It considers point-like H_2 molecules, due to the low eccentricity of the ellipsoid of the real molecule, and it has been shown that reproduces quite accurately the equation of state of bulk solid H_2 . The corrugation effects induced by the substrate were introduced by taking into account all the C- H_2 individual interactions, that are assumed to be of Lennard-Jones type with parameters taken from Ref. 13. All the above sets of parameters were used both for graphene and graphite alike, the only difference in their respective simulations being the number of graphene sheets considered in the calculation of the C- H_2 interaction potential. Following the results of Ref. 8, we modeled graphite by a series of 8 parallel graphene layers separated by a distance of 3.35 \AA from each other and stacked in the A-B-A-B form characteristic of this compound. The presence of additional carbon layers did not modify the H_2 binding energies to the substrate, the results for 8 and 9 carbon sheets being equivalent within their error bars.

III. RESULTS

We started our study by comparing the experimentally obtained binding energies e'_b s in the infinite dilution limit to the ones calculated by means of the DMC technique described above. This was done for graphite, since there is no experimental data for graphene yet. The results are $e_b = -482.7 \pm 3.5$ K (experimental, Ref. 14) versus -482.57 ± 0.06 K (this work). The good agreement between both values means that the C- H_2 potential used here is expected to give accurate results for this system. The energy obtained for graphene was -431.79 ± 0.06 K, i.e., a difference with the previous case of 50.78 ± 0.08 K.

Our main goal was to calculate the phase diagram of the first layer of H_2 on top of both graphene and graphite until the experimental density for promotion to the second layer, 0.0937\AA^{-2} ¹⁵ and compare the results obtained. The first step towards this end is reported in Fig. 1, where we show the energies per particle of a liquid phase on top of graphene (black boxes) and graphite

(open boxes). Even though the liquid phase will be shown to be metastable, it is useful to calculate its properties from a methodological point of view, for the sake of comparison with other possible phases and previous calculations. In both cases, we used the same simulation cell of $34.43 \times 34.08 \text{\AA}^2$, with a variable number of H_2 molecules on top of it to match the densities displayed in the figure. Periodic boundary conditions were considered for the x and y directions. To aid in the comparison, the results for graphite were up-shifted by the difference in the binding energies in the infinite dilution limit between graphene and graphite, given in the last paragraph. Since the error bars are of the size of the symbols, we can see that both curves are virtually identical. This is confirmed by a look to the results displayed in Table I, that come from least-squared fitting with cubic polynomials to the DMC data displayed in Fig. 1. The equilibrium densities ρ_0 in graphene and graphite are equal within error bars, and the difference between the energies per molecule at equilibrium e_0 is ~ 0.3 K after having considered the shifting due to the differences in the substrate. These results indicate that in the metastable liquid phase, the main difference between graphene and graphite as adsorbents is a nearly constant shift in the binding energies, as in

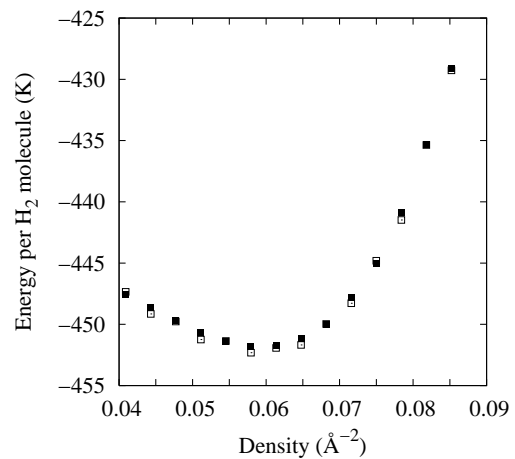


FIG. 1: Energy per H_2 molecule in the metastable liquid phase for graphene (full boxes) and graphite (open boxes). To afford an easy comparison, this latter results are up-shifted by the difference between the binding energies of a single hydrogen molecule on top of graphene and graphite.

TABLE II: Density and energy per H_2 molecule for the incommensurate triangular solids obtained by least squared fits to the simulation results. Graphene (2D) and graphite (2D) indicate the results after the subtraction of their respective energies in the infinite dilution limit, as in the previous table. The 2D entries are results for different calculations of pure 2D H_2 systems.

	Graphene	Graphite	Graphene (2D)	Graphite (2D)	2D (Ref. 16)	2D (Ref. 27)	2D (Ref. 28)
$e_0(K)$	-454.1 ± 0.3	-505.2 ± 0.2	-22.3 ± 0.3	-22.6 ± 0.2	-23.453 ± 0.003	-22.1 ± 0.1	-23.25 ± 0.05
$\rho_0 (\text{\AA}^{-2})$	0.0689 ± 0.0005	0.0689 ± 0.0006	0.0689 ± 0.0005	0.0689 ± 0.0006	0.0673 ± 0.0002	0.064 ± 0.01	0.0668 ± 0.0005
$\rho_s (\text{\AA}^{-2})$	0.0606 ± 0.0001	0.0600 ± 0.0001	0.0606 ± 0.0001	0.0606 ± 0.0001	0.0584 ± 0.0001	-	0.059 ± 0.001

the case of ^4He .⁸ The spinodal densities ρ_s , defined as the points in which the derivative of the pressure with respect to the surface density equals zero, are also indistinguishable in both cases. We can compare the results obtained for the liquid phase with the ones for a purely two dimensional (2D) system. In Ref. 16, this was made in the same conditions that the ones considered here, i.e., with the same intermolecular potential and for $T = 0$ K, as corresponds to a DMC calculation; their results are shown in Table I for comparison. We can infer that the introduction of both corrugation and movement in a perpendicular direction to the basal plane have the effect of decreasing the binding energy of the liquid at zero pressure (21.43 for a flat surface versus around 20 K for graphene and graphite).

Experimental data of H_2 on top of graphite^{15,17-19} indicate that the liquid phase is metastable with respect to both the incommensurate and commensurate solids, as in the ^4He case. This feature is confirmed by the present results shown in Fig. 2, where we display the energies of H_2 on graphene for its liquid (full boxes), commensurate $\sqrt{3} \times \sqrt{3}$ structure (open circle, density 0.0636 \AA^{-2}), and incommensurate triangular solid phases (open boxes). The dotted line is a least-squares fit to DMC data for the latter phase with a third degree polynomial. From Fig. 2, we conclude that the ground state of H_2 on top of

graphene is a $\sqrt{3} \times \sqrt{3}$ commensurate (C) solid, as it is on graphite, whose phase diagram is similar and not shown for simplicity. The binding energies per H_2 molecule for this C solid are -461.12 ± 0.01 and -512.97 ± 0.02 K for graphene and graphite, respectively. Their difference (51.85 K) is slightly larger than the one for the binding energy in the infinite dilution limit (50.78 K), indicating that the additional stabilization due to the extra graphite layers is more important for the C solid phase (1.07 versus 0.37 K). The energy of the C phase for graphite is slightly below the variational results of Novaco²¹ for the same structure (-510.8 K). Since the binding energy of this commensurate phase is always larger than the one corresponding to the liquid phase, we conclude that for densities smaller than 0.0636 \AA^{-2} the system will break in H_2 patches separated by empty space to produce the average density we could be interested in.

In order to establish the minimum density for which the incommensurate (IC) solid is stable we should make a double-tangent Maxwell construction between the C and IC phases. Since the C phase is defined by a single density, the construction was made by drawing the tangent line to the IC equation of state that intersects the C point. The result is depicted in Fig. 3 for the case of graphene. There, we can see that the limiting density for the IC solid in equilibrium with the $\sqrt{3} \times \sqrt{3}$

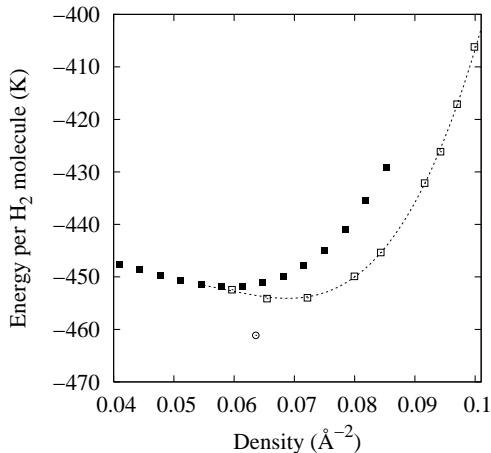


FIG. 2: Adsorption energy of H_2 on graphene. Full boxes, liquid metastable phase; open boxes, incommensurate triangular solid; open circle, commensurate $\sqrt{3} \times \sqrt{3}$ registered solid.

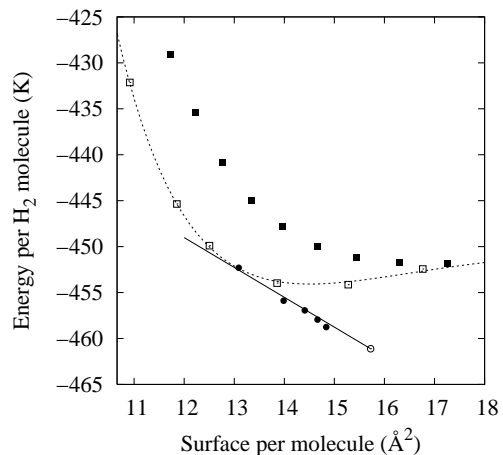


FIG. 3: Same than in previous figure but including the data for the α phase (full circles). The x-axis represents now the inverse of the density. The error bars are of the size of the symbols and not displayed for simplicity.

TABLE III: Energy per H₂ molecule for different arrangements found in the phase diagram of D₂ on graphite and its corresponding values for an incommensurate triangular solid at the same density. All data correspond to graphene.

Phase	ρ (Å ⁻²)	e_{binding} (K)	e_{IC} (K)
δ	0.0789	-442.22 ± 0.08	-450.88 ± 0.1
ϵ	0.0835	-440.30 ± 0.04	-446.47 ± 0.1
γ	0.0814	-441.24 ± 0.06	-448.76 ± 0.1

structure is 0.077 Å⁻² (the inverse of a limiting surface per molecule of 13 Å²), in excellent agreement with the available experimental data for graphite¹⁷⁻¹⁹ between 9 and 20 K (0.077 ± 0.001 Å⁻² ~ 1.22 times the density of the C phase). The binding energy corresponding to this structure is -452.08 K. The lower density for graphite is exactly the same, with a binding energy of -503.15 K. Obviously, to draw the limits of this transition is only possible if we consider corrugation in the graphene and graphite structures. The limits for this C-IC transition were not calculated quantitatively in any of the previous works of H₂ on graphite.²¹⁻²⁶ There have been also other calculations on the equation of state for a triangular solid in a purely 2D environment, both at zero¹⁶ and finite temperature.^{27,28} Their main results are summarized in Table II and compared to the present results for the IC solid. However, in the context of H₂ adsorption on graphene and graphite these strictly 2D results only serve as a check of the quality of our calculations, since the equilibrium density of the triangular 2D solid is below the IC density limit determined by the Maxwell construction (Fig. 3).

We have also analyzed the possible existence of the so-called α phase, or striped domain phase, in adsorbed H₂. According to experiments in graphite,^{18,20} it consists of strips of the C phase of variable width separated by narrow walls in which the H₂ molecules are closer to each other (see the phase diagrams in Ref. 18). This phase is also present in D₂,²⁹ and appears in the phase diagram drawn in Ref 25. The α structure can be defined by a rectangular cell that contains more or less H₂ molecules depending on the width of the C domains. In Fig. 3, we display as solid circles the cases for 4,6,8,10 and 12 molecules per simulation cell. It can be seen that they are approximately on top of the Maxwell construction line that limits the C-IC transition. This result implies that we can consider the α phase as intermediate between them, with continuous changes from the C to the α phase, and from the α to the IC solid, at least at $T = 0$ K. This continuous change is in agreement with the experimental

results of Cui *et al.*,²⁰ which ruled out a first order change between the C and the α arrangement. However, our results do not allow us to determine if the α phase is a real thermodynamical phase or simply a mixture of the C and IC phases separated by striped domains. The reason is that the simulation results are below but too close to the Maxwell construction line for making a definitive commitment (see Fig. 3). The data for graphite are similarly basically on top of the corresponding Maxwell construction line, and can be obtained from the graphene ones in Fig. 3 by applying a downward shift of 51.46 K.

To complete the study of H₂ on top of graphene, we checked the existence of three hypothetical phases that appear in the experimental²⁹ phase diagram of D₂ on top of graphite and that have not been experimentally observed in H₂. Two of them are commensurate: the ϵ phase, which is a 4 × 4 structure ($\rho = 0.0835$ Å⁻²), and the δ phase, which corresponds to a $5\sqrt{3} \times 5\sqrt{3}$ arrangement ($\rho = 0.0789$ Å⁻²). Both of them are within the density limits corresponding to the IC triangular phase. In D₂ on graphite, there is also an incommensurate oblique phase, which is called the γ phase, whose range of stability is approximately between 0.077 and 0.083 Å⁻². We calculated the corresponding energies per particle for the above mentioned commensurate phases and for a single density of the γ phase (0.0814 Å⁻²), and compared them to the energies of an IC triangular phase at the same densities. The results are displayed in Table III. The main conclusion is that for H₂ all these arrangements are metastable with respect to the incommensurate solid.

IV. CONCLUDING REMARKS

Summarizing, we have studied the phase diagram of H₂ on top of graphene using the most powerful microscopic tool at zero temperature (DMC), accurate potentials, and incorporating explicit C-H₂ interactions (fully corrugated model). The phase diagram of the first layer on graphene is fully determined for the first time. The ground state corresponds to a $\sqrt{3} \times \sqrt{3}$ commensurate solid as happens in ⁴He.⁸ Graphene and graphite show basically the same phase diagram, the main difference being the adsorption energy, which is ~ 51 K larger in graphite.

We acknowledge partial financial support from the Junta de Andalucía group PAI-205, DGI (Spain) Grant No. FIS2008-04403 and Generalitat de Catalunya Grant No. 2009SGR-1003.

¹ K.S. Novoselov, A.K. Geim, S.V. Morozov, D. Jiang, Y. Zhang, S.V. Dubonos, I.V. Grigorieva, and A.A. Firsov, *Science* **306**, 666 (2004).

² K.S. Novoselov, D. Jiang, F. Schedin, T.J. Booth, V.V.

Khotkevich, S.V. Morozov, and A.K. Geim, *PNAS* **102**, 10451 (2005).

³ C.H. Lui, L. Liu, K.F. Mak, G.W. Flynn, and T.F. Heinz, *Nature (London)* **462**, 339 (2009).

- ⁴ K.S. Novoselov, A.K. Geim, S.V. Morozov, D. Jiang, M.I. Katsnelson, I.V. Grigorieva, S.V. Dubonos, and A.A. Firsov, *Nature (London)* **438**, 197 (2005).
- ⁵ Y. Zhang, Y. Tan, H.L. Stormer, and P. Kim. *Nature (London)* **438**, 201 (2005).
- ⁶ C. Berger, Z. Song, T. Li, X. Li, A.Y. Ogbazghi, R. Feng, Z. Dai, A.N. Marchenkov, E.H. Conrad, P.N. First, and W.A. Heer, *J. Phys. Chem B.* **108**, 19912 (2004).
- ⁷ A.K. Geim and K.S. Novoselov, *Nat.Mat.* **6**, 183 (2007).
- ⁸ M.C. Gordillo and J. Boronat, *Phys. Rev. Lett.* **102**, 085303 (2009).
- ⁹ D.S. Greywall and P.A. Busch, *Phys. Rev. Lett.* **67**, 3535 (1991).
- ¹⁰ D.S. Greywall, *Phys. Rev. B* **47**, 309 (1993).
- ¹¹ J. Boronat and J. Casulleras, *Phys. Rev. B* **49**, 8920 (1994).
- ¹² I. F. Silvera and V. V. Goldman, *J. Chem. Phys.* **69**, 4209 (1978).
- ¹³ G. Stan and M.W. Cole, *J. Low Temp. Phys.* **110**, 539 (1998).
- ¹⁴ G. Vidali, G. Ihm, H.Y Kim, and M.W. Cole, *Sur. Sci. Reports* **12**, 135 (1991).
- ¹⁵ L.W. Bruch, M.W. Cole, and E. Zaremba, *Physical adsorption: forces and phenomena*, Oxford University Press, Oxford (1997).
- ¹⁶ C. Cazorla and J. Boronat, *Phys. Rev. B.* **78**, 134509 (2008).
- ¹⁷ H. Freimuth and H. Wiechert, *Surf. Sci.* **162**, 432 (1985).
- ¹⁸ H. Freimuth and H. Wiechert, *Surf. Sci.* **189/190**, 548 (1987).
- ¹⁹ H. Wiechert, *Physica B* **169**, 144 (1991).
- ²⁰ J. Ciu and S.C. Fain, Jr. *Phys. Rev. B* **39** 8628 (1989).
- ²¹ A.D. Novaco, *Phys. Rev. Lett.* **60**, 2058 (1988).
- ²² X.Z. Ni and L.W. Bruch, *Phys. Rev. B* **33**, 4584 (1986).
- ²³ J.M. Gottlieb and L.W. Bruch, *Phys. Rev. B* **40**, 148 (1989).
- ²⁴ K. Nho and E. Manousakis, *Phys. Rev. B* **65**, 115409 (2002).
- ²⁵ K. Nho and E. Manousakis, *Phys. Rev. B* **67**, 195411 (2003).
- ²⁶ E. Vives and P.A. Lindgard. *Phys. Rev. B* **47** 7431 (1993).
- ²⁷ M.C. Gordillo and D.M. Ceperley, *Phys. Rev. Lett.* **79**, 3010 (1997).
- ²⁸ M. Boninsegni, *Phys. Rev. B* **70**, 193411 (2004).
- ²⁹ H. Freimuth, H. Wiechert, H.P. Schildberg, and H.J. Lauter *Phys. Rev. B.* **42**, 587 (1990).